Water Supply

IWA PUBLISHING

Water Supply Vol 23 No 12, 5004 doi: 10.2166/ws.2023.309

Insights into karst groundwater hydrogeochemical characteristics and spatial evolution in the Jinan karst aquifer system, northern China

Dan Liu[a,b], Chanjuan Tian[a,b], Xuequn Chen[a,b,*], Wenjing Zhang[c], Xin Zhang[a,b], Zezheng Wang[c], Dandan Xu[a,b] and Yawen Chang[a,b]

[a] Water Resources Research Institute of Shandong Province, Jinan 250013, China
[b] Shandong Provincial Key Laboratory of Water Resources and Environment, Jinan 250013, China
[c] College of New Energy and Environment, Jilin University, Changchun 130021, China
*Corresponding author. E-mail: cxq1115@126.com

ABSTRACT

Karst aquifers are strategically important as they supply domestic water and are a resource for irrigation and industry in northern China. The heterogeneity of the karst aquifer medium makes it vulnerable to external influences. Here, samples of surface water and groundwater in a typical karst groundwater system of Jinan (China) were collected in December 2021, and the sample data were analyzed to further elucidate the hydrogeochemical processes. Results showed that the predominant water chemical type is HCO_3-Ca, with a lesser proportion of type HCO_3·SO_4-Ca and SO_4-Ca. The dominant water–rock interactions comprise the dissolution of carbonate minerals, gypsum, and halite and ion exchange. Dissolution/precipitation of calcite, dolomite, and gypsum determines the concentrations of Ca^{2+}, Mg^{2+}, HCO_3^-, and SO_4^{2-}. In terms of spatial distribution, the indirect and direct recharge areas are dominated by calcite dissolution, followed by dolomite dissolution, and are prone to ion exchange. The hydrogeochemical formation mechanism of the discharge area is more complicated by other hydrochemical processes and anthropogenic activities. These results provide guidance for global karst groundwater resource management and pollution prevention.

Key words: evolution process, hydrogeochemical characteristic, Jinan basin, karst groundwater, water–rock interaction

HIGHLIGHTS

- Study the scientific issues to be solved in the research of hydrogeological characteristics in the process of karst groundwater circulation in Jinan.
- Enrich the technical connotation of karst groundwater resource management and pollution prevention.

1. INTRODUCTION

Karst groundwater is an important component of regional water sources and it has become the primary water resource for meeting human demand in many areas (Ford & Williams 1989; C. S. Li *et al.* 2018; Yang *et al.* 2019). Approximately 20%–25% of the world's population depends on karst groundwater for potable water (Ma *et al.* 2011; Ford & Williams 2007; Lin *et al.* 2019). It is therefore important to study the hydrogeochemical characteristics and spatial evolution of karst groundwater before appropriate environmental protection measures can be taken (Frank *et al.* 2018; Wu *et al.* 2020).

The particular hydrogeological characteristics of a karst system, together with the high heterogeneity, openness, and high vulnerability of the aquifer (Bakalowicz 2005; Ghezelayagh *et al.* 2021), make karst groundwater particularly sensitive to external environmental influences (Eftimi *et al.* 2017; Hao *et al.* 2021). Generally, the hydrogeochemical characteristics of karst groundwater are controlled by many processes such as climate change (Berner 1992), land use (Sullivan *et al.* 2019), aquifer minerals (Williams 1993), and anthropogenic activities (such as agricultural activities and domestic sewage etc.) (Moral *et al.* 2008; Nguyen *et al.* 2014). Therefore, the interaction between surface water and karst groundwater and the influence of hydrochemical formation in the process of groundwater flow need to be fully elucidated (Eftimi *et al.* 2017; Basack *et al.* 2022; Raji & Packialakshmi 2022). Recently, hydrochemical methods have been widely employed as an important means to investigate hydrogeochemical characteristics (Nguyen *et al.* 2014). In Guizhou Province, China, Hao *et al.* (2021) utilized hydrochemical methods to determine the seasonal variation of chemical properties and define the water

quality. Martos-Rosillo & Moral (2015) revealed the hydrochemical changes due to the intensive use of karst groundwater in Seville, southern Spain, in order to achieve its sustainable use. However, further research is needed to better understand how the hydrochemical characteristics of groundwater near rivers are formed.

Jinan City, located in a typical karst area in the semiarid region of northern China, has karst groundwater as its essential source of water supply (Chen *et al.* 2021). Numerous previous studies on the karst groundwater resource of Jinan City have focused on the groundwater flow (Qian *et al.* 2006; Wang *et al.* 2016), hydrologic processes (Kang *et al.* 2011; Zhang *et al.* 2018), spring formation (Zhang *et al.* 2018; Luo *et al.* 2020), and hydrochemical characteristics (Wu *et al.* 2020). Over past decades, with the development of industry and agriculture, the continuous increase in the utilization of the karst groundwater resource has led to a decline in the groundwater level and deterioration of groundwater quality (Schöpke *et al.* 2017; C. S. Li *et al.* 2018; Luo *et al.* 2020; Zhang & Wang 2021).

The components of the karst groundwater system of Jinan comprise the indirect recharge area (IRA), direct recharge area (DRA), and discharge area (DA) (Chen *et al.* 2021). The hydrogeochemical characteristics of karst groundwater are controlled by the recharge, runoff, and discharge conditions (Wu *et al.* 2009). Earlier research on the Jinan spring area has focused mainly on the DA, which is always preferentially selected for groundwater development. However, along the general path of groundwater flow, the ion concentrations change due to water–rock interactions between the groundwater and the aquifer materials. It is important to identify differences in the hydrogeochemical characterization of karst groundwater between the recharge area and the DA; however, previous research has largely focused on the environmental quality of karst groundwater, while ignoring the spatial variation of karst groundwater (Wang *et al.* 2006).

For the hydrogeochemical processes, it is understandable that the spatial hydrogeochemical characteristics and evolution processes of the Jinan karst groundwater system could be very different from the spatial distribution. This motivates us to collect samples from IRA, DRA, and DA and conduct this investigation, and several methods including hydrochemical analysis, Piper diagram, Gibbs diagram, the ion ratio method, and statistical analysis were applied to answer the following three questions: (1) What are the hydrogeochemical characteristics of karst groundwater and how do they differ from those of surface water? (2) What water–rock interactions control the formation and evolution of karst groundwater? (3) What are the spatial differences in karst groundwater within the study area and how are they manifested? The objectives of this study were to identify the hydrogeochemical characteristics of karst groundwater and to provide a reference for both the management of karst groundwater and the exploration of effective methods for karst groundwater development and utilization.

2. MATERIALS AND METHODS

2.1. Study area

The study area is located in the Jinan karst aquifer system, Shandong Province, China (Figure S1, Supplementary Information). This region has a tropical semiarid continental monsoon climate, with an average annual precipitation of 698 mm, and an average annual evaporation of 1,476 mm, and an average annual temperature of 14.3 °C.

The study area is located on the northern wing of the western Luxi anticline, which is a gentle monoclinal structure. The terrain is high in the southeast and low in the northwest, changing from low hills, to remnant hills, and to piedmont plain landforms. The strata are inclined to the north and northwest, with an inclination of 5°–12°. From top to bottom, the main strata in this area are Quaternary, Tertiary, Carboniferous, Permian, Ordovician, Paleozoic Cambrian, and the Archaean Taishan Group of ancient metamorphic rock. In the northern part, there is an igneous rock mass intrusion of the Yanshanian period.

Karst groundwater generally flows from the south toward the north and is mainly controlled by topography and bounded by the watershed. The main aquifers of the sampling wells used in this study are the middle Cambrian Zhangxia Group, upper Cambrian Fengshan Group, and Ordovician aquifers. The aquifers consist of mainly carbonate rock fissure water, and the lithology is mainly limestone, dolomitic limestone, and argillaceous limestone. The karst groundwater system of Jinan is divided into IRA, DRA, and DA with different recharge sources and flow characteristics.

2.2. Sample collection and analysis

In December 2021, 20 water samples were collected for analysis, which comprised six groups of surface water from the Yufu River (labeled SW), 13 groups of karst groundwater (labeled KG), and one group of Heihu spring (labeled S-1). The distribution of sample points considers the hydrodynamic characteristics of the groundwater and the IRA, DRA, and DA (Figure S1).

Prior to sampling, all bottles were washed and rinsed thoroughly with water. The SW samples were collected directly. Most KG samples were obtained from wells after purging for at least 5 min; however, the KG-3 (artesian discharge well) and KG-14 (spring) samples were collected directly. All samples were filtered through 0.45 μm membrane filters immediately after collection and stored at 4 °C until laboratory analysis, which was conducted within a week of collection.

Field parameters, such as alkalinity, pH, total dissolved solids (TDS), electrical conductivity (EC), and dissolved oxygen (DO), were measured on-site using a multi-index portable meter (DZS-708; INSEA, China), which was calibrated using standard solutions prior to use. Major cations (i.e., Na^+, K^+, Ca^{2+}, and Mg^{2+}) and anions (i.e., SO_4^-, Cl^-, NO_3^-, and NO_2^-) were analyzed using ion chromatography (IC883; Metrohm, Switzerland), and HCO_3^- was determined by titration. Total organic carbon (TOC) was determined using a Shimadzu TOC-VCPH analyzer. The water samples used for cationic analysis were acidified to pH < 2 with ultrapure nitric acid and stored in polyethylene bottles. All chemical analyses were performed at Shandong Provincial Key Laboratory of Water Resources and Environment.

2.3. Data processing and statistical analysis

To qualitatively evaluate the potential variation in the equilibrium between minerals and water and in the trends in water–rock interactions (Clark 2015), the saturation index (SI) was calculated using PHREEQC as follows (Equation (1)):

$$\mathrm{SI} = \log \frac{\mathrm{IAP}}{K_{\mathrm{SP}}} \tag{1}$$

where IAP is the ion activity product and K_{SP} is the solubility product. In this study, $SI_{calcite}$, $SI_{dolomite}$, SI_{gypsum}, and SI_{halite} were determined by PHREEQC and are listed in Table S2.

The chloro-alkaline index (CAI) can be used to identify the ion exchange process between the groundwater and its surrounding environment during its migration and retention. The equations for calculating the CAI can be expressed as (all values in meq/L):

$$\mathrm{CAI}\quad \mathrm{I} = \frac{Cl^- - (Na^+ + K^+)}{Cl^-}, \tag{2}$$

$$\mathrm{CAI}\quad \mathrm{II} = \frac{Cl^- - (Na^+ + K^+)}{SO_4^{2-} + HCO_3^- + CO_3^{2-} + NO_3^-} \tag{3}$$

The correlation analysis was conducted to identify the relationships among the various hydrogeochemical compositions. Multivariate principal component analysis (PCA) was performed using ORIGIN 2022 to determine the primary factors that influence the hydrogeochemical characteristics.

3. RESULTS AND DISCUSSION

3.1. Characteristics of hydrochemical parameters

The on-site indicators and hydrochemical parameters of the SW and KG samples were analyzed and the results are listed in Tables S1 and S2. The Piper diagram of all samples divided into six zones is shown in Figure 1 and most samples fall in Zone 2 and Zone 5. The hydrochemical type of all SW samples and some KG samples is HCO_3–Ca, while the type of other KG samples is $HCO_3 \cdot SO_4$–Ca. The hydrochemical type of sample KG-3 is SO_4–Ca. With respect to cations, all samples fall in Zone B (Ca type), reflecting the prominence of carbonate weathering. With respect to anions, most samples fall in Zone F (HCO_3) and Zone H (mixed type), although one sample falls in Zone E (SO_4 type), representing the dominance of carbonate weathering and dissolution of gypsum. Generally, the hydrochemical type of KG shows consistency with that of SW, and this hydrochemical similarity suggests that they are related and probably have a close transformation relationship and hydraulic connection. According to previous research (Wu *et al.* 2020), the hydrochemical type of karst groundwater evolves from HCO_3–Ca to $HCO_3 \cdot SO_4$–Ca. The main reason for the difference in the current study is that the sampling sites are mostly located along the Yufu River, which is affected substantially by surface water recharge.

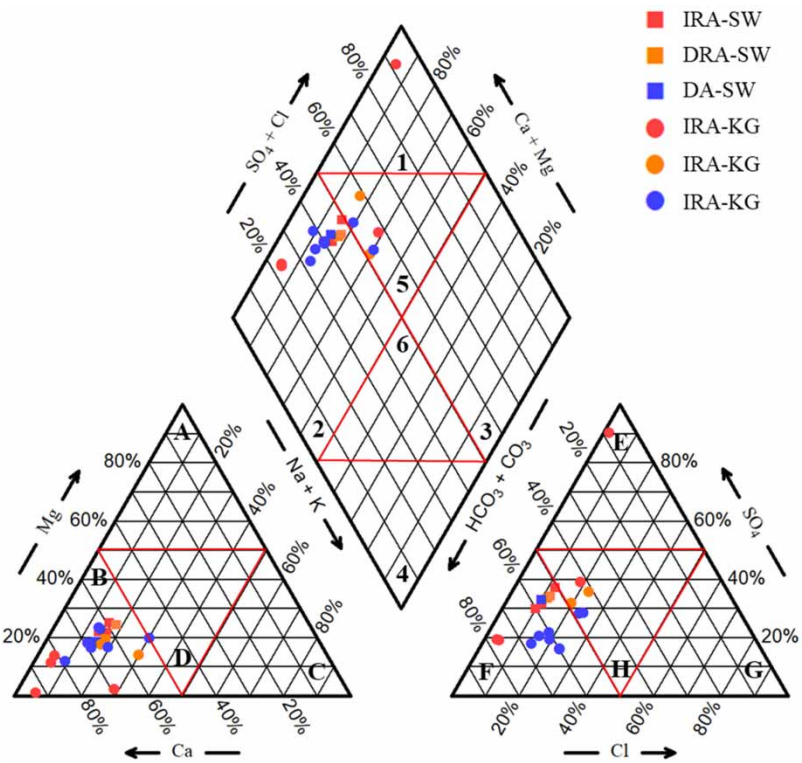

Figure 1 | Piper diagram of all water samples.

3.2. Evidence of major hydrochemical formation

A Gibbs diagram represents the equivalence ratios of $Na^+/(Na^+ + Ca^{2+})$ and $Cl^-/(Cl^- + HCO_3^-)$ as a function of TDS, which can be used to assess the natural sources of dissolved chemical constituents and investigate how chemical constituents form, including precipitation dominance, rock weathering dominance, and the evaporation–crystallization process (Gibbs 1971; Talib *et al.* 2019). Figure 2 shows that rock weathering contributes to the main process that controls the chemical composition of the groundwater. The $c(Na^+)/c(Na^+ + Ca^{2+})$ and $c(Cl^-)/c(Cl^- + HCO^{3-})$ values are <0.5, indicating that the anions and ions are mainly composed of HCO_3^- and Ca^{2+} (Huang *et al.* 2017). The main karst aquifers within the study area are Ordovician and Cambrian carbonates and therefore weathering dissolution of tuffs and dolomites occurs (Wang *et al.* 2016). There

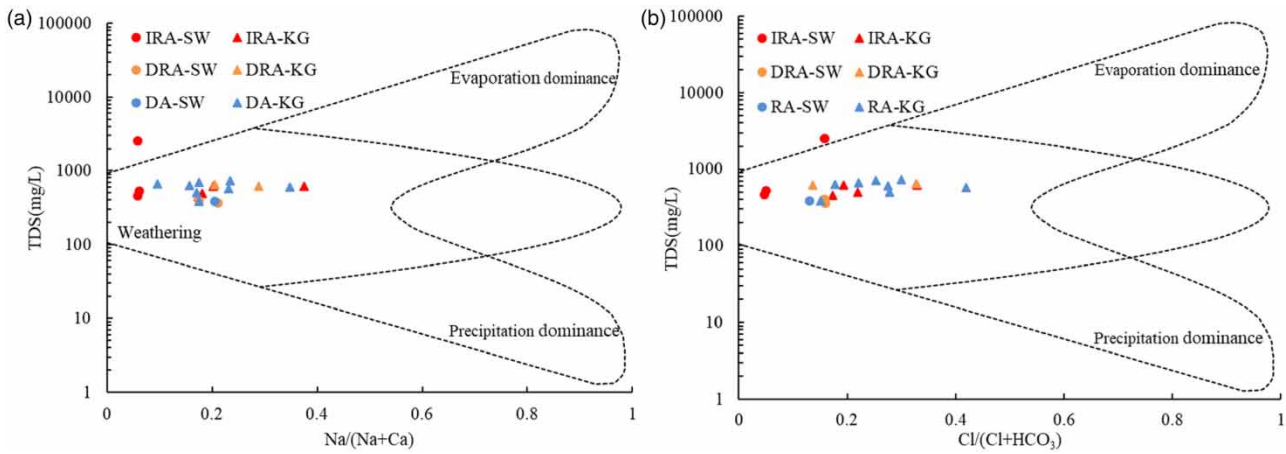

Figure 2 | Gibbs diagram: (a) $Na^+/(Na^+ + Ca^{2+})$ (mg/L) versus log TDS (mg/L) and (b) $Cl^-/(Cl^- + HCO_3^-)$ (mg/L) versus log TDS (mg/L).

is no substantial change in TDS with an increase in $c(Na^+)/c(Na^+ + Ca^{2+})$, showing that ion exchange also affects the chemical compositions by increasing Na^+ and decreasing Ca^{2+} (Su *et al.* 2023).

3.3. Evolution process between hydrochemistry and lithology of karst rocks

3.3.1. Ion exchange

Ion exchange is an important natural process that affects the contents of Ca^{2+} and Na^+ (Han *et al.* 2013; Lin *et al.* 2019). As can be seen in Figure 3(a), the relationship between $(Na^+ + K^+ - Cl^-)$ and $[(Ca^{2+} + Mg^{2+}) - (HCO_3^- + SO_4^{2-})]$ is linear with a slope value close to −1, which suggests Ca^{2+} and Mg^{2+} exchange with Na^+ adsorbed on the rock (X. X. Li *et al.* 2018). Almost all samples are located above the −1:1 line, indicating that Na^+ and Ca^{2+} in groundwater might have been affected by the dissolution of albite and anorthite, in addition to ion exchange. The samples in the DA deviate far from the −1 line, suggesting that anthropogenic input or reverse ion exchange might have increased the contents of Ca^{2+} and Mg^{2+}.

As can be seen in Figure 3(b), the CAI-1 and CAI-2 of most samples in the IRA and the DRA are <0, indicating that forward ion exchange leads to increase in Na^+ and decrease in Ca^{2+} (Equation (4)). However, the CAI of some KG samples in the DA are >0, signifying that reverse ion exchange is an important source of ions (Equation (5)). Ultimately, Ca^{2+} and Mg^{2+} in the aquifer are exchanged with Na^+ and K^+ in the groundwater (Yang *et al.* 2016; Wang *et al.* 2017).

$$CaSO_4 \cdot 2H_2O \rightarrow Ca^{2+} + SO_4^{2-} + 2H_2O \tag{4}$$

$$Na_2SO_4 \cdot 10H_2O \rightarrow 2Na + SO_4^{2-} + 10H_2O \tag{5}$$

3.3.2. Rock weathering

With consideration of the range values of carbonate rock, silicate rock, and halite, the effect of water–rock interaction on the water chemical composition was evaluated. As shown in Figure 4(a) and 4(b), carbonate weathering plays a crucial role in controlling the main hydrogeochemical characteristics of the water. Most KG samples in the IRA and DA are located close to carbonate rock, indicating that the ionic composition of groundwater in the IRA and DA is mainly affected by carbonate rock decomposition, especially in the IRA.

The HCO_3^-/Ca^{2+} value of all SW and KG samples in the DRA and DA is close to 1 (Figure 4(c)), indicating that dissolved calcite is dominant in producing Ca^{2+} and HCO_3^-. With increase in concentration, some KG samples in the IRA and DA fall below the 1:1 line, indicating that Ca^{2+} is released by reactions other than carbonate dissolution, e.g., gypsum. Meanwhile, the HCO_3^-/Mg^{2+} value of most samples falls between the 1:2 line and the 1:3 line (Figure 4(d)), indicating that dolomite minerals are the important source of Ca^{2+} and Mg^{2+} in DRA and DA, which aligns with previous studies (Su *et al.* 2023). The IRA-KG samples fall above the 1:3 line, indicating other sources of Mg^{2+}. The reasonable correlation between

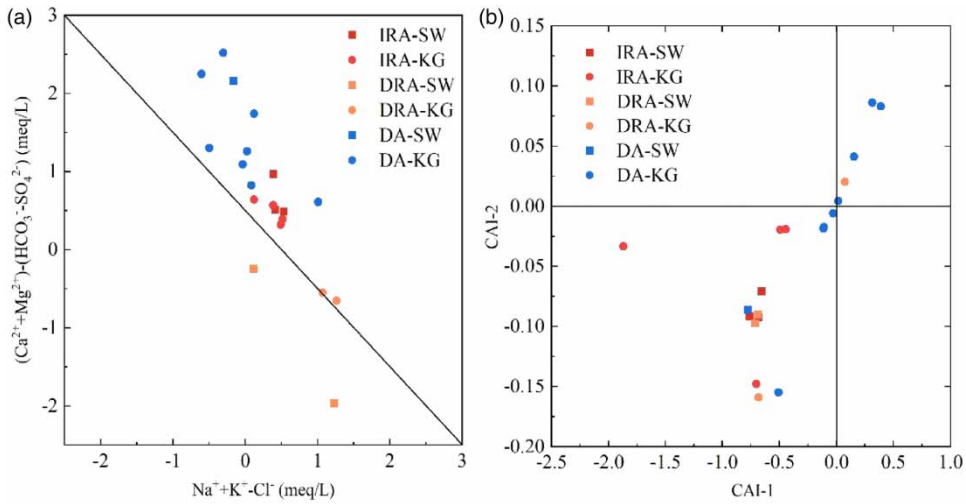

Figure 3 | Plots of (a) $(Ca^{2+} + Mg^{2+}) - (HCO_3^- + SO_4^{2-})$ versus $(Na^+ + K^+) - Cl^-$, and (b) CAI-1 versus CAI-2 indices of water in the study area.

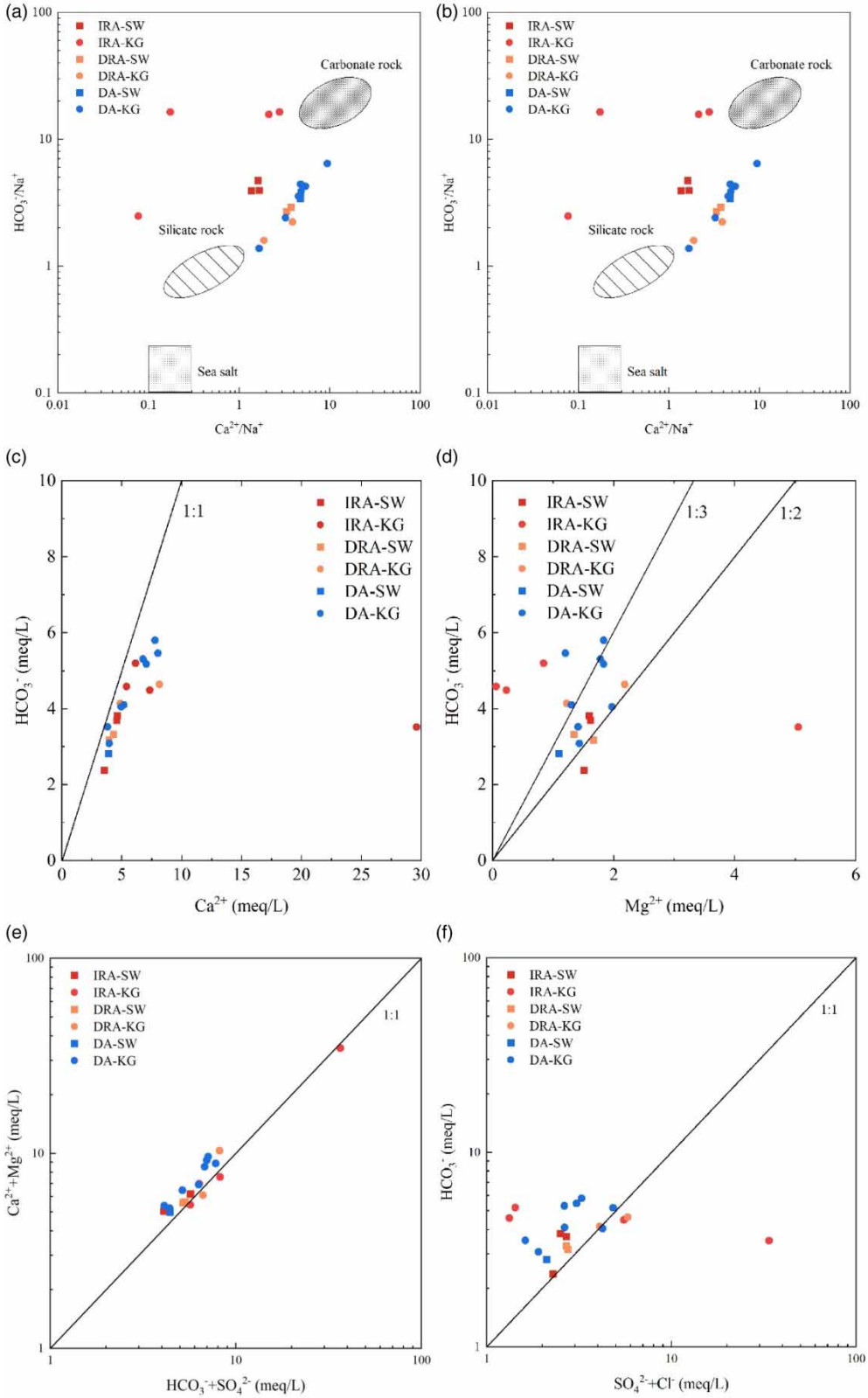

Figure 4 | Ion ratios characterizing the hydrogeochemical reactions in different water. (*continued.*).

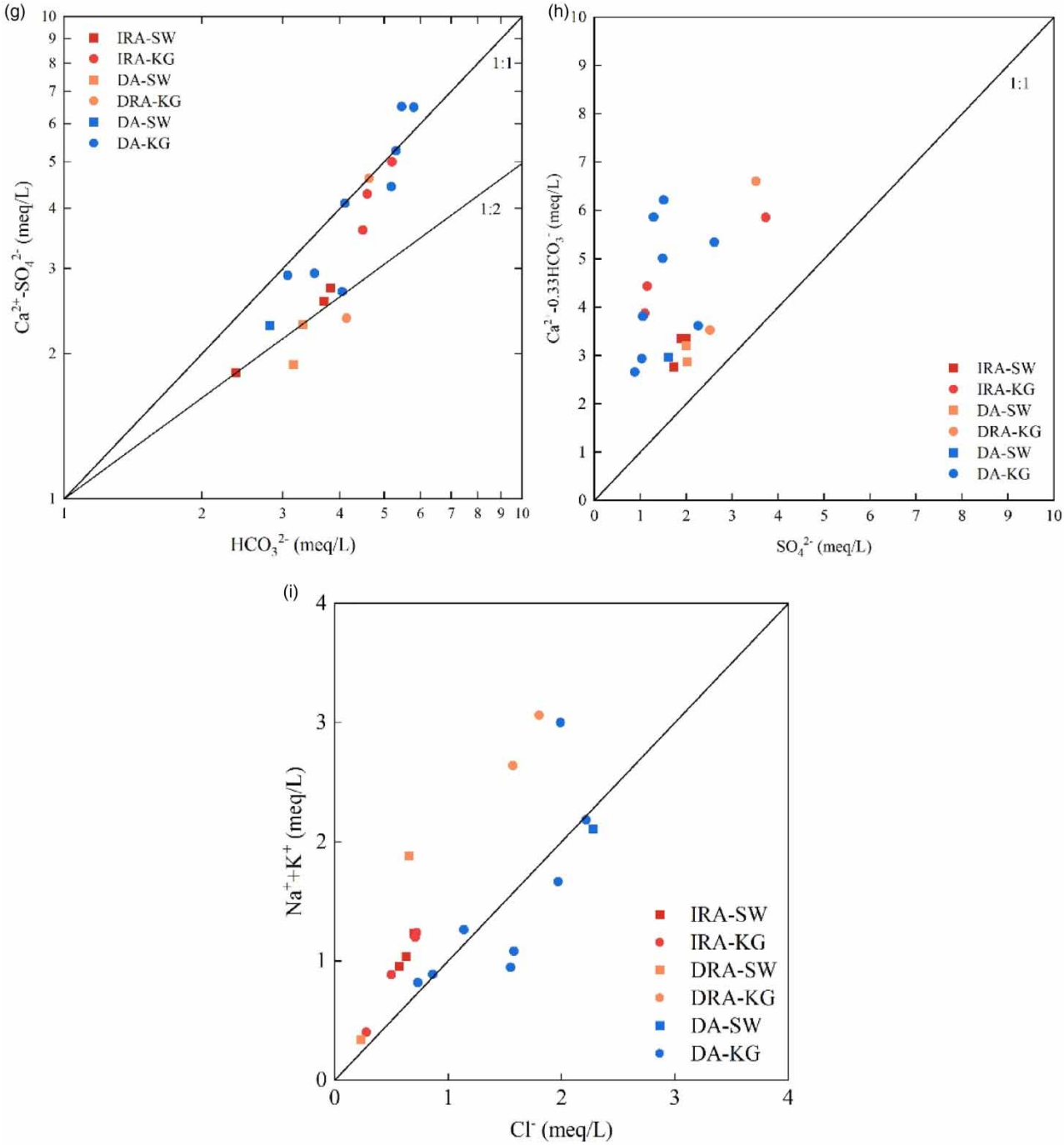

Figure 4 | Continued.

$Ca^{2+} + Mg^{2+}/HCO_3^- + SO_4^{2-}$ (Figure 4(e)) suggests that the dissolution of both carbonate and sulfate plays an important role (Wu *et al.* 2009). Samples in the IRA and DA are slightly above the 1:1 line, indicating that dissolution of carbonate is the main process of ion exchange (Dehnavi *et al.* 2011; Senthilkumar & Elango 2013), whereas samples in the DRA are slightly below the 1:1 line, which might be related to reverse ion exchange and sulfate reduction that causes the decrease in Ca^{2+} and Mg^{2+} (Zhang *et al.* 2020). In Figure 4(f), most samples are above the 1:1 line, indicating that the formation of the hydrochemical components of karst groundwater is attributable mainly to the dissolution of carbonate rocks, and partly in association with evaporate dissolution in some instances.

The effects of 'non-gypsum source calcium' and 'non-carbonate source calcium' on the hydrochemistry of karst water are shown in Figure 4(g) and 4(h) (Wang *et al.* 2006). In Figure 4(g), the KG samples are distributed mainly between the 1:1 line and the 1:2 line, whereas the SW samples are located mostly near the 1:2 line. The results show that the Ca^{2+} and HCO_3^- of the KG samples are mainly from dissolved calcite, followed by dolomite, while the SW samples are mainly from dissolved calcite. The KG samples are on the right of the plot, indicating that dolomite dissolution is enhanced. As evident in Figure 4(h), most samples are scattered above the 1:1 line, indicating that Ca^{2+} and SO_4^{2-} originate primarily from the dissolution of gypsum (Wu *et al.* 2014). With an increase in Ca^{2+}, the DA KG samples deviate further from the 1:1 line, indicating the presence of Ca^{2+} from non-hydropetrogenic sources in the karst water, which might be related to precipitation and anthropogenic activities (Wang *et al.* 2006).

Most of the KG samples in the DA areas are located along the 1:1 line in Figure 4(i), indicating that halite dissolution is the main source of Na^+ and Cl^-, especially for Cl^- (Yang *et al.* 2016). The excess of Cl^- over Na^+ in the DA KG samples indicates additional sources of chloride. On the one hand, reverse ion exchange might have occurred to reduce Na^+, which would explain the slight excess of Ca^{2+} and Mg^{2+} over SO_4^{2-} and HCO_3^- (Bakalowicz 1994). On the other hand, the characteristics of groundwater recharge and discharge represent other important influences on the content of Cl^- (Xanke *et al.* 2015). This further explains the deviation of $Ca^{2+} + Mg^{2+}$ in Figure 4(e) of the DA KG samples. Most samples in the IRA and DRA are above the 1:1 line, indicating that Na^+ has sources other than halite mineral dissolution. Guo *et al.* (2020) found the same conclusion in the closed karst groundwater basin of Jinan. This result is consistent with the content of Figure 3, which indicates that ion exchange might have occurred in the IRA and DRA.

3.3.3. Saturation indices

It can be seen from Figure 5(a) that most $SI_{calcite}$ values are >0, and that the $SI_{calcite}$ of the KG samples is greater than that of the SW samples, indicating that calcite is in a saturated state. The $SI_{dolomite}$ of the SW samples is <0, whereas the $SI_{dolomite}$ of most KG samples is >0, indicating that precipitation of dolomite occurs in groundwater (Figure 5(b)). Wang *et al.* (2006) reported that the dissolution rate of calcite is higher than that of dolomite, and that dolomite might still dissolve when calcite is oversaturated in KG, resulting in calcite precipitation. However, this is not consistent with the increase in Ca^{2+} (Figure 4(c)), which is due to gypsum in the aquifer, whereby the dissolution of gypsum leads to an increase in Ca^{2+}. When Ca^{2+} reaches a specified level, de-dolomitization will occur. The precipitation of calcite leads to a decrease in HCO_3^-, such that the dolomite is unsaturated and Mg^{2+} increases (Appelo & Postma 2005).

SI_{gypsum} is in the range of -1.97 to -0.03 (Figure 5(c)), indicating an unsaturated state of gypsum, whereby more gypsum dissolves in the water with groundwater flow. This is in marked contrast to the findings of other research in karst areas in China (Lin *et al.* 2019) and is related to dolomite dissolution and preferential exchange of Mg^{2+} by Ca^{2+}. SI_{halite} is also unsaturated, indicating the presence of halite dissolution (Figure 5(d)). SI_{gypsum} and SI_{halite} increase with an increase in TDS, indicating that the Ca^{2+}, SO_4^{2-}, Na^+, and Cl^- are from the dissolution of gypsum and halite. There is a notable relationship between $SI_{dolomite}$ and $SI_{calcite}$ (Figure 5(e)) that indicates that the composition of dolomite and decomposition of calcite are synchronous, which is in agreement with the results of analysis of the main ion sources (Wang *et al.* 2017).

From the IRA, DRA, and DA, there is no substantial change in $SI_{calcite}$. Dolomite is further dissolved and transitioned from the unsaturated state to the saturated state, and gypsum and halite are unsaturated. SI_{halite} in the DA is greater than that in the IRA, and SI_{gypsum} shows a trend of decrease (Deng *et al.* 2023). This indicates that groundwater has a strong ability to dissolve gypsum in the DA (Han *et al.* 2015).

3.4. Source similarity analysis of hydrogeochemical formation

PCA was used to elucidate the sources and influences of groundwater chemistry. According to Figure 6, the degree of similarity among SW samples is high, but there are some differences among the KG samples, indicating the influence of hydrochemical processes. The PC1 axis shows that TH, TDS, Ca^{2+}, Mg^{2+}, and SO_4^{2-} all contribute substantially, together accounting for 42.9% of the total. It shows that the dilution effect of ions related to limestone and gypsum dissolution is caused by karst groundwater evolution, evidenced by the close negative correlation of PC1 with pH, DO, TOC, and DO. Closely related to PC2 are alkalinity, Na^+, Cl^-, HCO_3^-, and NO_3^-, suggesting that the dissolution of halite and anthropogenic effects have a substantial impact on the hydrogeochemical characteristics (Cao *et al.* 2016).

Pearson correlation analysis represents the major contributions of ions to the groundwater totals and reveals the importance of certain effects (Figure S4). Alkalinity is correlated negatively with pH ($r > 0.5$) and correlated positively with

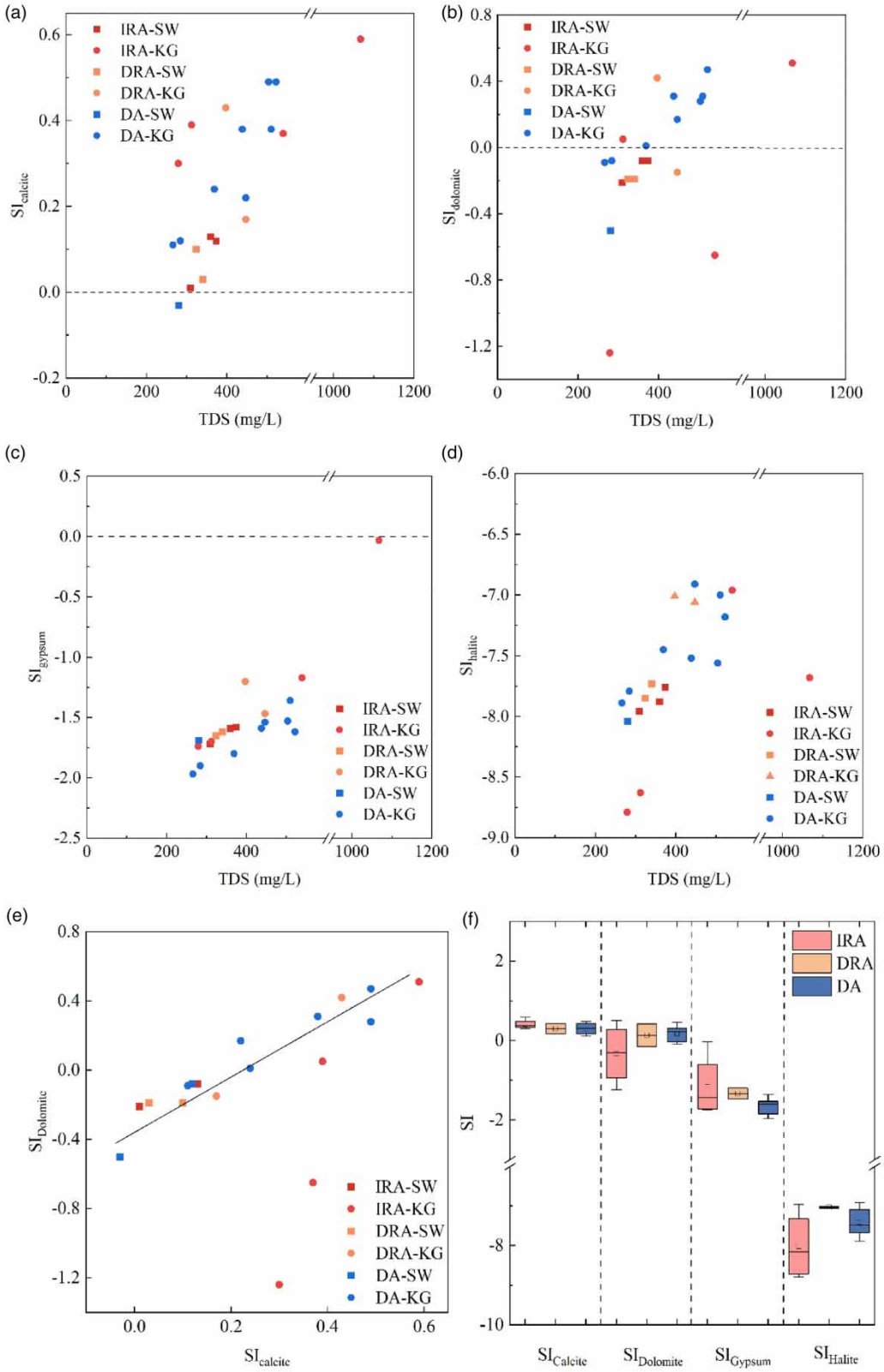

Figure 5 | Water sample saturation indices (SI) for (a) calcite, (b) dolomite, (c) gypsum, (d) halite, (e) $SI_{dolomite}$ versus $SI_{calcite}$, and (f) SI values in the IRA, DRA, and DA.

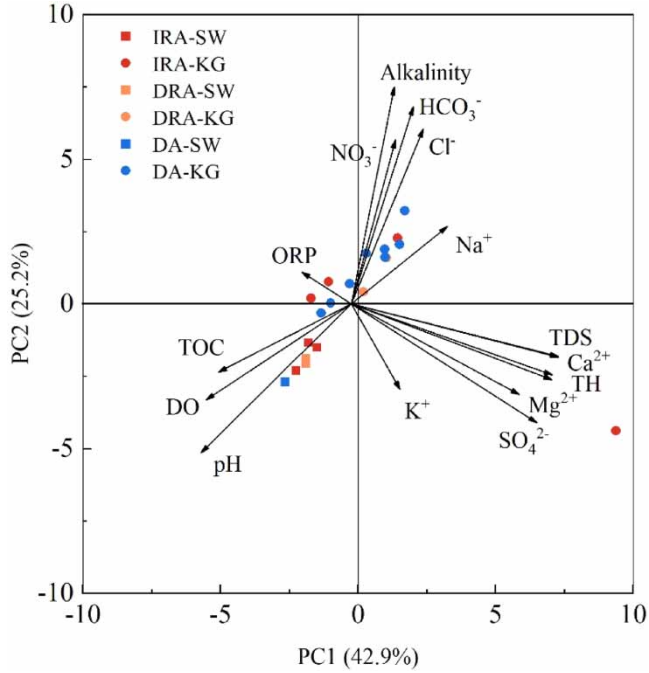

Figure 6 | PCA results showing relationships between water samples and hydrogeochemical parameters in terms of spatial variation.

HCO_3^- ($r > 0.9$). There are strong correlations between TDS and Ca^{2+}, Na^+, HCO_3^-, and SO_4^{2-}, with the most significant correlations between TDS and Ca^{2+} and SO_4^{2-}. Water–rock interactions control the composition of TDS, which is consistent with the results of the Gibbs analysis. There are moderate correlations between Ca^{2+} and HCO_3^- and SO_4^{2-}, because the main source of ions is related to the dissolution of dolomite, limestone, and gypsum. The results show that the weathering and dissolution of carbonate rock and sulfate minerals play important roles in controlling the chemical composition (Zhou *et al.* 2015). The aquifer in the Jinan spring area is mainly composed of limestone and dolomite, although some rock layers are mixed with gypsum. This is consistent with the ion ratio analysis results (Figure 5(c)). A strong correlation between Cl^- and Na^+ indicates that Cl^-, derived mainly from pollutants, increases the ionic strength of the karst groundwater, leading to strong dissolution of halite (Wang *et al.* 2023). There is also a positive correlation between EC and NO_3^-, indicating that anthropogenic activities cause an increase in NO_3^- in groundwater. Moreover, NO_3^- has a significant correlation with Cl^- ($r = 0.78$), which shows that NO_3^- pollution promotes the accumulation of Cl^-.

4. CONCLUSIONS

Hydrochemistry provided important information about the hydrogeochemical characteristics of a karst groundwater system in Jinan and revealed the evolution processes in IRA, DRA, and DA in Jinan, Shandong Province. The major conclusions drawn are as follows:

(1) The hydrochemical type of SW and KG is predominantly HCO_3–Ca, but the type of some samples is $HCO_3 \cdot SO_4$–Ca and SO_4–Ca. The ion content is higher in the DRA and DA than in the IRA. This is mainly influenced by rock weathering and ion exchange in the aquifer, and especially by human activities such as agriculture in the DRA.

(2) The process and extent of rock weathering cause differences in the IRA, DRA, and DA, mainly due to different flow paths and residence times, which indicate the extent of groundwater circulation. Ca^{2+}–SO_4^{2-}/HCO_3^- and Ca^2–0.33 HCO_3^-/SO_4^{2-} as the monitoring tracer provide additional insight into the evolution process. Groundwater in the DRA is readily saturated with calcite, but unsaturated with gypsum, and the dissolution of gypsum minerals leads to de-dolomitization. Groundwater in the IRA and DA is mainly affected by the decomposition of carbonate rock, especially in the IRA.

(3) The groundwater in the DRA is recharged by the IRA and has experienced a longer path. The increase in salinity is mainly controlled by the dissolution of gypsum and halite minerals. The groundwater in the IRA and DRA is more vulnerable to pollution discharges. In addition to ion exchange and rock weathering, there are other hydrochemical processes that supply notable amounts of SO_4^{2-} and Na^+. The mechanisms affecting groundwater chemistry in the study area are still largely controlled by geogenic processes rather than by anthropogenic activities.

In addition, we emphasize the need for future studies to assess the differences in hydrogeochemical characteristics between different regions, and for targeted work to be undertaken to develop and protect groundwater resources.

AUTHORS CONTRIBUTIONS

D. L. and X. C. are responsible for the formulation and methodology of overarching research aims. C. T. analyzed the major hydrochemical formation. W. Z. and Z. W. analyzed the major ion sources and hydrogeochemical evolution. X. Z. and D. X. performed the principal component analysis. Y. C. performed the Pearson correlation analysis. All authors read and approved the final manuscript.

FUNDING

This research was funded by the Natural Science Foundation of Shandong Province (ZR2021QD031; ZR2021MD086), Water Conservancy Technology Demonstration Project (SF-202210), Optional Subjects of the Water Resources Research Institute of Shandong Province (SDSKYZX202121-1) and the Key Technology and Application Project of Flood Control and Waterlogging Control in Plain Waterlogging Depression (PCTXPQ-KY202001-2).

DATA AVAILABILITY STATEMENT

All relevant data are included in the paper or its Supplementary Information.

CONFLICT OF INTEREST

The authors declare there is no conflict.

REFERENCES

Appelo, C. A. J. & Postma, D. 2005 *Geochemistry, Groundwater and Pollution*. Taylor & Francis, London, UK.

Bakalowicz, M. 1994 Water geochemistry: water quality and dynamics. In: *Groundwater Ecology* (Gibert, J., Danielopol, D. L. & Stanford, J. A., eds), Academic Press, San Diego, CA, USA, pp. 97–127.

Bakalowicz, M. 2005 Karst groundwater: a challenge for new resources. *Hydrogeology Journal* **13**, 148–160.

Basack, S., Goswami, G., Khabbaz, H. & Karakouzain, M. 2022 Flow characteristics through granular soil influenced by saline water intrusion: a laboratory investigation. *Civil Engineering Journal* **8** (5), 863–878.

Berner, R. A. 1992 Weathering, plants, and the long-term carbon cycle. *Geochimica et Cosmochimica Acta* **56** (8), 3225–3231.

Cao, G., Scanlon, B. R., Han, D. & Zheng, C. 2016 Impacts of thickening unsaturated zone on groundwater recharge in the North China Plain. *Journal of Hydrology* **537**, 260–270.

Chen, X. Q., Guan, Q. H., Li, F. L., Liu, D., Han, C. H. & Zhang, W. J. 2021 Study on the ecological control line in the major leakage area of Baotu spring in Shandong Province, eastern China. *Ecological Indicators* **133**, 108467.

Clark, I. 2015 *Groundwater Geochemistry and Isotopes*. CRC Press, Boca Raton, FL, USA.

Dehnavi, A. G., Sarikhani, R. & Nagaraju, D. 2011 Hydrogeochemical and rock water interaction studies in east of Kurdistan, N-W of Iran. *International Journal of Environmental Science and Research* **1**, 16–22.

Deng, X., Xing, L. T., Zhang, F. J., Xing, X. R., Zhang, Y. F., Yu, M., Liu, S. Z. & Pan, W. Y. 2023 Mapping regional and nested flow systems in the karst aquifers of Jinan spring using hydrochemical and isotope data. *Water Supply* **23** (8), 3323–3344.

Eftimi, R., Akiti, T., Amataj, S., Benishke, R., Zojer, H. & Zoto, J. 2017 Environmental hydrochemical and stabile isotope methods used to characterise the relation between karst water and surface water. *Acque Sotterranee – Italian Journal of Groundwater* **6** (1), 7–20.

Ford, D. C. & Williams, P. W. 1989 *Karst Geomorphology and Hydrology*. Springer, Dordrecht, The Netherlands.

Ford, D. & Williams, P. W. 2007 *Karst Hydrogeology and Geomorphology*. Wiley, Hoboken, USA.

Frank, S., Goeppert, N. & Goldscheider, N. 2018 Fluorescence-based multi-parameter approach to characterize dynamics of organic carbon, faecal bacteria and particles at alpine karst springs. *Science of the Total Environment* **615**, 1446–1459.

Ghezelayagh, P., Javadi, S. & Kavousi, A. 2021 COP*KAT: a modified COP vulnerability mapping method for karst terrains using KARSTLOP factors and fuzzy logic. *Environmental Earth Sciences* **80** (17), 592.

Gibbs, R. J. 1971 Mechanisms controlling world water chemistry. *Science* **172** (3985), 871–872.

Guo, Y. L., Zhang, C., Xiao, Q. & Bu, H. 2020 Hydrogeochemical characteristics of a closed karst groundwater basin in North China. *Journal of Radioanalytical and Nuclear Chemistry* **325** (2), 365–379.

Han, Y., Wang, G. C., Cravotta III, C. A., Hu, W. Y., Bian, Y. Y., Zhang, Z. W. & Liu, Y. Y. 2013 Hydrogeochemical evolution of Ordovician limestone groundwater in Yanzhou, North China. *Hydrological Processes* **27** (16), 2247–2257.

Han, Z. W., Tang, C. Y., Wu, P., Zhang, R. X., Zhang, C. P. & Sun, J. 2015 Hydrogeochemical characteristics and associated mechanism based on groundwater dating in a karstic basin, Guizhou Province, China. *Environmental Earth Sciences* **73** (1), 67–76.

Hao, Z., Gao, Y., Green, S. M., Wen, X. F., Yang, J., Xiong, B. L., Quine, T. A. & He, N. P. 2021 Chemical characteristics of flow driven by rainfall and associated impacts on shallow groundwater quality in a karst watershed, Southwest China. *Environmental Processes* **8** (2), 615–636.

Huang, X., Wang, G., Liang, X., Cui, L., Ma, L. & Xu, Q. 2017 Hydrochemical and stable isotope (δD and δ^{18}O) characteristics of groundwater and hydrogeochemical processes in the Ningtiaota coalfield, northwest China. *Mine Water and the Environment* **37** (1), 119–136.

Kang, F. X., Jin, M. G. & Qin, P. R. 2011 Sustainable yield of a karst aquifer system: a case study of Jinan springs in northern China. *Hydrogeology Journal* **19**, 851–863.

Li, C. S., Wu, X. C., Sun, B., Sui, H. B., Geng, F. Q., Qi, H. & Ma, X. Y. 2018 Hydrochemical characteristics and formation mechanism of geothermal water in northern Ji'nan. *Earth-Science* **43** (S1), 313–325.

Li, X. X., Wu, P., Han, Z. W., Zha, X. F., Ye, H. J. & Qin, Y. J. 2018 Effects of mining activities on evolution of water quality of karst waters in Midwestern Guizhou, China: evidences from hydrochemistry and isotopic composition. *Environmental Science and Pollution Research* **25** (2), 1220–1230.

Lin, Y., Ren, H. X., Wu, Y. Z., Cao, F. L. & Qu, P. C. 2019 The evolution of hydrogeochemical characteristics of a typical piedmont karst groundwater system in a coal-mining area, Northern China. *Environmental Earth Sciences* **78** (18), 557.

Luo, Q. K., Yang, Y., Qian, J. Z., Wang, X. X., Chang, X., Ma, L., Li, F. L. & Wu, J. F. 2020 Spring protection and sustainable management of groundwater resources in a spring field. *Journal of Hydrology* **582**, 124498.

Ma, R., Wang, Y. X., Sun, Z. Y., Zheng, C. M., Ma, T. & Prommer, H. 2011 Geochemical evolution of groundwater in carbonate aquifers in Taiyuan, northern China. *Applied Geochemistry* **26** (5), 884–897.

Martos-Rosillo, S. & Moral, F. 2015 Hydrochemical changes due to intensive use of groundwater in the carbonate aquifers of Sierra de Estepa (Seville, Southern Spain). *Journal of Hydrology* **528**, 249–263.

Moral, F., Cruz-Sanjulián, J. J. & Olías, M. 2008 Geochemical evolution of groundwater in the carbonate aquifers of Sierra de Segura (Betic Cordillera, southern Spain). *Journal of Hydrology* **360** (1–4), 281–296.

Nguyen, T. T., Kawamura, A., Tong, T. N., Nakagawa, N., Amaguchi, H. & Gilbuena, R. 2014 Hydrogeochemical characteristics of groundwater from the two main aquifers in the Red River Delta, Vietnam. *Journal of Asian Earth Sciences* **93**, 180–192.

Qian, J. Z., Zhan, H. B., Wu, Y. F., Li, F. L. & Wang, J. Q. 2006 Fractured-karst spring-flow protections: a case study in Jinan, China. *Hydrogeology Journal* **14**, 1192–1205.

Raji, V. R. & Packialakshmi, S. 2022 Assessing the wastewater pollutants retaining for a soil aquifer treatment using batch column experiments. *Civil Engineering Journal* **8** (7), 1482–1491.

Schöpke, R., Preuß, V., Zahn, L., Thürmer, K., Walko, M. & Totsche, O. 2017 Control of the remediation of anoxic AMD groundwater by sulphate reduction in subsoil reactor. In: *13th International Mine Water Association Congress – Mine Water & Circular Economy*, June 25–30, Lappeenranta, Finland.

Senthilkumar, M. & Elango, L. 2013 Geochemical processes controlling the groundwater quality in lower Palar river basin, southern India. *Journal of Earth System Science* **122** (2), 419–432.

Su, C., Zhang, X. Q., Sun, Y. W., Meng, S. H., Cui, X. X. & Fei, Y. H. 2023 Hydrochemical characteristics and evolution processes of karst groundwater in Pingyin karst groundwater system, North China. *Environmental Earth Sciences* **82**, 67.

Sullivan, P. L., Macpherson, G. L., Martin, J. B. & Price, R. M. 2019 Evolution of carbonate and karst critical zones. *Chemical Geology* **527**, 119223.

Talib, M. A., Tang, Z., Shahab, A., Siddique, J., Faheem, M. & Fatima, M. 2019 Hydrogeochemical characterization and suitability assessment of groundwater: a case study in central Sindh, Pakistan. *International Journal of Environmental Research and Public Health* **16** (5), 886.

Wang, Y. X., Guo, Q. H., Su, C. L. & Ma, T. 2006 Strontium isotope characterization and major ion geochemistry of karst water flow, Shentou, northern China. *Journal of Hydrology* **328**, 592–603.

Wang, J. L., Jin, M. G., Lu, G. P., Zhang, D. L., Kang, F. X. & Jia, B. J. 2016 Investigation of discharge-area groundwaters for recharge source characterization on different scales: the case of Jinan in northern China. *Hydrogeology Journal* **24** (7), 1723–1737.

Wang, L. H., Dong, Y. H., Xu, Z. F. & Qiao, X. 2017 Hydrochemical and isotopic characteristics of groundwater in the northeastern Tengger Desert, northern China. *Hydrogeology Journal* **25** (8), 2363–2375.

Wang, K. R., Wu, Z., Fu, S. D., Qiu, Y. T. & Chen, H. W. 2023 Hydrochemical evolution and genesis analysis of karst water system in Jinan Basin. *Geochimica. Feochimica* **52** (5), 547–558. (in Chinese).

Williams, P. W. 1993 Environmental change and human impact on karst terrains. In: *Karst Terrains: Environmental Changes and Human Impact* (Williams, P. W., ed.), Catena Verlag, Cremlingen, Germany, pp. 1–19.

Wu, P., Tang, C., Zhu, L., Liu, C., Cha, X. & Tao, X. 2009 Hydrogeochemical characteristics of surface water and groundwater in the karst basin, Southwest China. *Hydrological Processes* **23** (14), 2012–2022.

Wu, J. H., Li, P. Y., Qian, H., Duan, Z. & Zhang, X. D. 2014 Using correlation and multivariate statistical analysis to identify hydrogeochemical processes affecting the major ion chemistry of waters: a case study in Laoheba phosphorite mine in Sichuan, China. *Arabian Journal of Geosciences* **7** (10), 3973–3982.

Wu, X. C., Li, C. S., Sun, B., Geng, F. Q., Gao, S., Lv, M. H., Ma, X. Y., Li, H. & Xing, L. T. 2020 Groundwater hydrogeochemical formation and evolution in a karst aquifer system affected by anthropogenic impacts. *Environmental Geochemistry and Health* **42** (9), 2609–2626.

Xanke, J., Goeppert, N., Sawarieh, A., Liesch, T., Kinger, J., Ali, W., Hötzl, H., Hadidi, K. & Goldscheider, N. 2015 Impact of managed aquifer recharge on the chemical and isotopic composition of a karst aquifer, Wala reservoir, Jordan. *Hydrogeology Journal* **23** (5), 1027–1040.

Yang, Q., Li, Z., Ma, H., Wang, L. & Martín, J. D. 2016 Identification of the hydrogeochemical processes and assessment of groundwater quality using classic integrated geochemical methods in the Southeastern part of Ordos Basin, China. *Environmental Pollution* **218**, 879–888.

Yang, P. H., Li, Y., Groves, C. & Hong, A. H. 2019 Coupled hydrogeochemical evaluation of a vulnerable karst aquifer impacted by septic effluent in a protected natural area. *Science of the Total Environment* **658**, 1475–1484.

Zhang, Z. & Wang, W. 2021 Managing aquifer recharge with multi-source water to realize sustainable management of groundwater resources in Jinan, China. *Environmental Science and Pollution Research* **28** (9), 10872–10888.

Zhang, Z. X., Wang, W. P., Qu, S. S., Huang, Q., Liu, S., Xu, Q. & Ni, L. D. 2018 A new perspective to explore the hydraulic connectivity of karst aquifer system in Jinan spring catchment, China. *Water* **10** (10), 1368.

Zhang, H. T., Xu, G. Q., Zhan, H. B., Chen, X. Q., Liu, M. C. & Wang, M. H. 2020 Identification of hydrogeochemical processes and transport paths of a multi-aquifer system in closed mining regions. *Journal of Hydrology* **589**, 125344.

Zhou, J., Xing, L. T., Zhang, F. J., Han, Z., Peng, T. Q., Xu, M. T. & Yang, Y. 2015 Chemical characteristics research on karst water in Jinan spring area. *Advanced Materials Research* **1092–1093**, 593–596.

First received 9 July 2023; accepted in revised form 12 November 2023. Available online 23 November 2023